the vexillum may be an adaptation to the echolocation system of glossophagine pollinators is supported by the fact that species of *Mucuna* that are visited by small palaeotropical Megachiropteran bats (which do not have an echolocating system) do not possess raised and concave vexilla[6,7]. We suggest that similar adaptations may have been evolved by other neotropical bat-pollinated plant species.

Dagmar von Helversen, Otto von Helversen
Zoological Institute, University of Erlangen, 91058 Erlangen, Germany
e-mail: helver@biologie.uni-erlangen.de

1. Dobat, K. *Blüten und Fledermäuse* (Kramer, Frankfurt, 1985).
2. von Helversen, O. in *Animal–Plant Interactions in Tropical Environments* (eds Barthlott, W. *et al.*) 41–59 (Museum Koenig, Bonn, 1993).
3. Vogel, S *Flora B* **158,** 185–222 (1969).
4. Baker, H. G. *Rev. Biol. Trop.* **17,** 187–197 (1970).
5. Tschapka, M. Thesis, Univ. Erlangen.
6. Hopkins, H. C. F. & Hopkins, M. J. G. *Kew Bull.* **48,** 297–306 (1993).
7. Grünmeier, R. in *Animal–Plant Interactions in Tropical Environments* (eds Barthlott, W. *et al.*) 29–39 (Museum Koenig, Bonn, 1993).

Cognitive restoration of reversed speech

Speech is the most complex auditory signal and requires the most processing[1]. The human brain devotes large cortical areas[2,3] to deciphering the information it contains, as well as parsing speech sounds produced simultaneously by several speakers[4]. The brain can also invoke corrective measures to restore distortions in speech[5]; for example, if a brief speech sound is replaced by an interfering sound that masks it, such as a cough, the listener perceives the missing speech as if the brain interpolates through the absent segment. We have studied the intelligibility of speech, and find it is resistant to time reversal of local segments of a spoken sentence, which has been described as "the most drastic form of time scale distortion"[6].

We subdivided a digitized sentence into segments of fixed duration (say, 50 ms). Every segment was then time-reversed without smoothing the transition borders between the segments. The entire spoken sentence was therefore globally contiguous, but locally time-reversed, at every point (A+B in Fig. 1). Listeners report perfect intelligibility of the sentence for segment durations up to 50 ms, and partial intelligibility for segment durations exceeding 100 ms (Fig. 1, bottom), with 50% intelligibility occurring at about 130 ms; by psychoacoustic standards, such segment distortions are very long. Many defining features of speech sounds are rapid temporal transitions with durations well within the reversal window.

Perception of speech against local time reversal is robust even if alternating segments are shifted in time (A+delayed B). Speech also remains intelligible if odd-numbered segments are displaced forwards in time by two or three times the duration of the window. For example, for segments of 100 ms, shifting the odd-numbered segment forward in time by 200 ms reduces the intelligibility rating by only 15%. For segments of 50 ms, intelligibility is not significantly affected by a displacement of 100 or 200 ms, but the speech does sound more echoic. Furthermore, the results are not changed if half the segments (A in Fig. 1) are presented to one ear and the other half (B in Fig. 1) to the other ear.

When subjects listen repeatedly to locally time-reversed sentences with moderately long windows (100 ms), they report that previously unintelligible words become clear. This type of 'learning' is not simply due to an improvement in identification, as subjects say they can now hear actual words, indicating some form of cognitive recalibration. The experience is similar to familiarization with a newly heard accent.

These findings lend support to recent theories[7,8] of speech encoding that state, contrary to conventional thinking, that a detailed auditory analysis of the short-term acoustic spectrum is not essential to the speech code. Rather, the ultralow-frequency modulation envelopes in the order of 3 to 8 Hz are critical cues to intelligibility. Although the amplitude spectrum of a waveform is unaffected by time reversal, the temporal envelopes, as well as the fine structure of the running spectrum, are highly distorted for such sounds. The

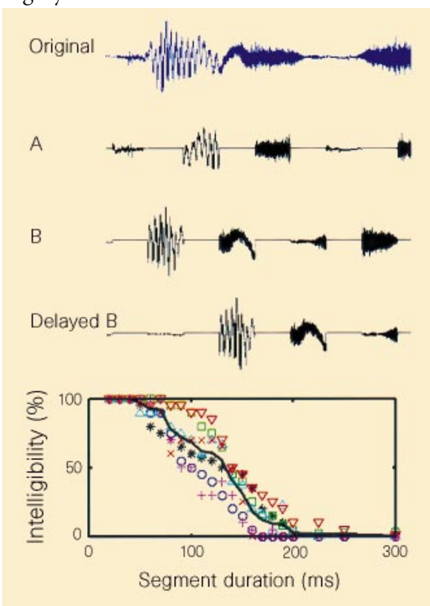

Figure 1 Segments of speech showing the effects of time reversal. Top, 50-ms segments of original and locally time-reversed (A+B) speech. Bottom, subjective intelligibility rating by seven subjects (different symbols). The solid line shows the average rating score.

advantage of a robust speech-encoding system that uses higher-order corrective measures and ultralow-frequency cues is obvious in noisy environments where the listener needs to extract perceptually and identify a stream of speech cues that compete with extraneous noise, as in the 'cocktail party effect'[9].

Kourosh Saberi*, David R. Perrott†
**Division of Biology 216-76, Caltech, Pasadena, California 91125, USA*
e-mail: kourosh@caltech.edu
†Department of Psychology, California State University, Los Angeles, California 90032, USA

1. Moore, B. C. J. *An Introduction to the Psychology of Hearing* 4th edn (Academic, New York, 1997).
2. Lassen, N. A., Ingvar, D. H. & Skinhoj, E. *Sci. Am.* **239,** 50–59 (1978).
3. Nishizawa, Y., Olsen, T. S., Larsen, B. & Lassen, N. *J. Neurophysiol.* **48,** 458–466 (1982).
4. Cherry, E. C. *J. Acoust. Soc. Am.* **25,** 975–979 (1953).
5. Warren, R. M., Bashford, J. A., Healy, E. W. & Brubaker, B. S. *Percept. Psychophys.* **55,** 313–322 (1994).
6. Licklider, J. C. R. & Miller, G. A. *The Perception of Speech. Handbook of Experimental Psychology* (ed. Stevens, S. S.) 1040–1074 (Wiley, New York, 1960).
7. Greenberg, S. & Arai, T. *J. Acoust. Soc. Am.* **103,** 3057 (1998).
8. Greenberg, S. I. *Behav. Brain Sci.* **21,** 267 (1998).
9. Yost, W. A. *Percept. Psychophys.* **58,** 1026–1036 (1996).

Co-carcinogenic effect of β-carotene

Epidemiological and animal studies on vitamin A and its analogues support the hypothesis that β-carotene can prevent cancer in humans[1]. However, chemoprevention trials have unexpectedly shown that β-carotene, either alone or in combination with vitamin A or vitamin E, actually increases lung-cancer incidence and mortality in heavy smokers and asbestos workers[2–4]. We find that β-carotene in rat lung produces a powerful booster effect on phase I carcinogen-bioactivating enzymes, including activators of polycyclic aromatic hydrocarbons (PAHs), and that this induction is associated with the generation of oxidative stress. Our findings might explain why β-carotene supplementation increases the risk of lung cancer in smokers.

The α-tocopherol β-carotene (ATBC) and β-carotene retinol efficacy trial (CARET) chemoprevention studies suggested that heavy smokers should avoid high-dose β-carotene supplements because of an increased risk of lung cancer[2–4]. The ATBC study (29,133 participants) recorded 18% more lung cancers and 8% more overall deaths in smokers taking β-carotene; in CARET (18,314 participants), there were 28% more lung cancers and 17% more deaths in smokers and asbestos workers who were taking β-carotene and vitamin A supplements. Rather than initiating new tumours, β-carotene might have co-carcinogenic properties on latent ones[5].

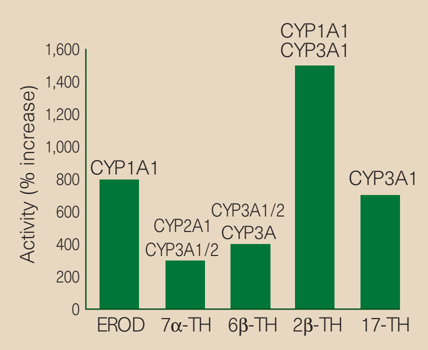

Figure 1 Enzymatic CYP induction by β-carotene. Male Sprague–Dawley rats (aged 6–7 weeks, 140 ± 10 g) maintained on a standard laboratory diet received by mouth daily 500 mg per kg body weight of β-carotene (Aldrich, Milan) for five consecutive days; controls received only corn oil. Because of species specificity, the purpose of the *in vivo* experiments was to find evidence of the co-carcinogenic potential of β-carotene[7], not to mimic a trial situation. Rats were fasted for 16 h before being killed humanely in accordance with approved procedures. Ten rats were in each group; lung microsomes were tested immediately for ethoxyresorufin *O*-deethylase (EROD) and testosterone hydroxylase[8] (TH).

Because β-carotene is known to be an antigenotoxic agent[6], we decided to investigate whether it might act by means of epigenetic mechanisms, such as those involving cytochrome P450 (CYP) changes[7].

We found a highly significant increase in the carcinogen-metabolizing enzymes CYP1A1/2 (activating aromatic amines, polychlorinated biphenyls, dioxins and PAHs), CYP3A (activating aflatoxins, 1-nitropyrene and PAHs), CYP2B1 (activating olefins and halogenated hydrocarbons) and CYP2A (activating butadiene, esamethyl phosphoramide and nitrosamines) in the lungs of rats supplemented with high doses of β-carotene. This was documented by marked increases in the following probes: ethoxyresorufin *O*-deethylase activity (CYP1A1-linked), testosterone 7α-hydroxylation (CYP1A1/2 and CYP2A1), 6β-hydroxylation (CYP1A1/2 and CYP3A1), 2β-hydroxylation (CYP1A1 and CYP3A1) and androst-4-ene-3,17-dione-associated monooxygenase (17-testosterone hydroxylase, CYP2B1 and CYP3A1) (Fig. 1).

In humans, correspondingly high levels of CYPs would predispose an individual to cancer risk from the widely bioactivated tobacco-smoke procarcinogens. Moreover, many of these could act synergistically with β-carotene as CYP inducers to impose a co-carcinogenic effect, particularly in genetically predisposed individuals who inherit the 'at risk' genotypes of xenobiotic metabolizing enzymes[9]. Indeed, studies have associated an increased risk of lung cancer with the induction of aryl hydrocarbon hydroxylase and/or polymorphisms in CYP1A1 (ref. 10). Although β-carotene is known to increase the levels of phase II detoxifying enzymes such as glutathione *S*-transferase Mu and glutathione peroxidase enzymes, smokers with the CYP1A1 exon-7 valine polymorphism have significantly higher levels of PAH–DNA adduct; β-carotene intake does not significantly decrease these levels[11].

We used electron paramagnetic resonance to evaluate the precise contribution of CYPs induced by β-carotene on superoxide production. There was a significant association between the induction of CYP content in subcellular lung preparations and the overgeneration of superoxide yield (not shown), which could act synergistically with the peroxyl radicals, nitrogen dioxide and hydroquinones that are contained in cigarette smoke. The pro-oxidant activity of β-carotene has also been unambiguously demonstrated at a high partial pressure of oxygen. Because this is highest in the outermost cells of the lung, these cells might be particularly subject to the pro-oxidant effect of β-carotene[12].

We found in a medium-term bioassay with BALB/c 3T3 cells that β-carotene enhances the conversion of the prototype benzo(*a*)pyrene to the ultimate carcinogens (our unpublished data). This co-carcinogenic activity of β-carotene is in line with the boosting effect of β-carotene itself on activating enzymes during cell growth.

Although cancer chemoprevention cannot rely merely on the control of antioxidants, there have been proposals to take advantage of the radical-trapping ability of β-carotene (and probably of other carotenoids) to try to decrease the incidence of lung cancer in humans. We postulate that the paradoxical effect of increased morbidity and mortality observed in the clinical chemoprevention trials is probably due to the co-carcinogenic properties of β-carotene and its ability to generate oxidative stress[13]. We think that our findings are relevant to public health policy and that they should be considered before widespread supplementation with these micronutrients is recommended.

M. Paolini*, G. Cantelli-Forti*, P. Perocco†, G. F. Pedulli‡, S. Z. Abdel-Rahman§, M. S. Legator§

**Department of Pharmacology, Biochemical Toxicology Unit, Via Irnerio 48, 40126 Bologna, Italy*
e-mail: paolini@biocfarm.unibo.it
†*Institute of Cancerology, Viale Filopanti 22, 40126 Bologna, Italy*
‡*Department of Organic Chemistry 'A. Mangini', Via S. Donato 15, 40127 Bologna, Italy*
§*Department of Preventive Medicine and Community Health, University of Texas Medical Branch, Galveston, Texas 77555-1110, USA*

1. Ziegler, R. G. *et al. J. Natl Cancer Inst.* **88,** 612–615 (1996).
2. The α-Tocopherol, β-Carotene Cancer Prevention Study Group *N. Engl. J. Med.* **330,** 1029–1035 (1994).
3. Omenn, G. S. *et al. J. Natl Cancer Inst.* **88,** 1550–1558 (1996).
4. Omenn, G. S. *et al. N. Engl. J. Med.* **334,** 1150–1155 (1996).
5. Hinds, T. S., West, W. L. & Knight, E. M. *Ther. Rev.* **37,** 551–558 (1997).
6. Azuine, M. A., Goswami, U. C., Kayal, J. J. & Bhide, S. V. *Nutr. Cancer* **17,** 287–295 (1992).
7. Paolini, M., Biagi, G., Bauer, C. & Cantelli-Forti, G. *Trends Pharmacol. Sci.* **15,** 322–323 (1994).
8. Paolini, M. *et al. Br. J. Pharmacol.* **122,** 344–350 (1997).
9. Bartsch, H. & Hietanen, E. *Environ. Health Perspect.* **104** (suppl. 3), 569–577 (1996).
10. Hayashi *et al. Jpn. J. Cancer Res.* **83,** 866–870 (1992).
11. Mooney, L. A. *et al. Carcinogenesis* **18,** 503–509 (1997).
12. Rice-Evans, C. A., Sampson, J., Bramley, P. M. & Holloway, D. E. *et al. Free Radical Res.* **26,** 381–398 (1997).
13. Rowe, P. M. *Lancet* **348,** 1369 (1996).

Growth of nanotubes for probe microscopy tips

Carbon nanotubes, which have intrinsically small diameters and high aspect ratios and which buckle reversibly, make potentially ideal structures for use as tips in scanning probe microscopies, such as atomic force microscopy (AFM)[1–4]. However, the present method of mechanically attaching nanotube bundles for tip fabrication is time consuming and selects against the smallest nanotubes, limiting the quality of tips. We have developed a technique for growing individual carbon nanotube probe tips directly, with control over the orientation, by chemical vapour deposition (CVD) from the ends of silicon tips. Tips grown in this way may become widely used in high-resolution probe microscopy imaging.

Our approach to growing individual nanotube probes involves flattening a conventional silicon (Si) tip at its apex by contact AFM imaging and anodizing it in hydrogen fluoride[5] to create nanopores of 50–100 nm diameter along the tip axis. Iron catalyst is electrodeposited into the pores from $FeSO_4$ solution[6], and nanotubes are grown by CVD with ethylene and hydrogen at 750 °C. The orientated pore structure was chosen for the catalyst support in order to control the direction of growth[7] and enable the reproducible production of nanotube tips for imaging.

CVD nanotube tips are formed reproducibly after a reaction lasting 10 min (Fig. 1). They are usually too long to be used as tips, and are shortened by an *in situ* AFM technique[1,2]. A typical field-emission scanning electron microscopy (FE-SEM) image of a nanotube tip after it was shortened and used for AFM imaging (Fig. 1a) shows a well-defined tube 480 nm long protruding from the Si tip apex. Nanotube tips produced under these conditions and viewed by FE-SEM have an average diameter of 10 ± 5 nm. Further characterization of these tips by transmission electron microscopy show that they are multi-walled nanotubes (MWNTs) with well-ordered graphene walls (Fig. 1b).

AFM measurements of the cantilever